

オープンMRI装置を配置した際に考えられる問題点の内、①外来電磁波ノイズ対策、②前述の画像診断装置が発生する干渉電磁波ノイズ対策、③オープンMRIの発生する漏洩磁場対策、④手術室の高耐床荷重対策、⑤高重量の画像機器の搬入方法、搬入経路などを検討し、設計に反映させた。

これらの検討結果を踏まえ、手術室構築のための設計を実施し、具体的な施工に繋がった。例えば、オープンMRIは重量が15トン強あるので、国立がんセンター中央病院9階の手術室フロアの大梁に、設置するMRIの3本の脚部の内2本を配置し、残りの脚部1本を、元の躯体の小梁を補強するために鉄骨を配置して荷重を耐えられるレベルとした。

また、自走式CT装置のレール部分の補強やFPD-DR装置のCアーム部の天井吊り部も、上部の補強鉄骨を配置し、地震等外力が働いても大丈夫な構造とした。

[II]内視鏡の画像は、画像周辺部に歪みが認められるが、今回開発した2段階補正処理により、画像周辺部の歪みがより高精度に補正されることを確認した。これにより内視鏡画像とCT画像、MRI画像とを重畳表示することが可能であることを示した。

具体的な各種手術の場面では、軟性内視鏡で、術野の中心部を確認しながら手術処置を実施するが、周辺部の状況確認には、CT、MRIで術前に撮像した3次元画像などを軟性内視鏡画像と重畳することで、手術の安全性を高め、効果的な手術を実現することが可能である。このように画像支援により、従来難しかった深部、狭小部、

臓器の背後など直視できない領域の手術を可能にすると思われる。

[III]手術用ロボット装置の根幹部である操作コンソールの概念を構築し、その基盤技術開発を実施した。手術プロトコルを想定し、主術者と補助術者のためのコンソールを用意することを想定して、その要素技術を開発した。ユーザビリティを想定し、グラフィカルユーザーインターフェイスを視認性の良いものとして構築すべく、その基礎的な画面や操作性などの検証を実施した。これにより、次年度より実施する開発をより効果的に進めることが出来ると思われる。

今後、マスタースレーブ方式の手術用具を開発し、それらと一体になった手術用ロボット装置を実現することが今後の課題となる。実際にマスター側とスレーブ側のインターフェイス、及びその制御プロトコルの統一化など実施すべき項目は多く、今後日立製作所機械研究所と密接なタイアップを実現し、効率よく研究開発を進められるように考えたい。

E. 結論

[I]今回の手術室環境構築の研究において、手術室内に設置の手術支援を実施する画像診断支援機器相互の干渉問題を解決することが今回の重要課題となった。特に、①外来電磁波ノイズ遮蔽対策、②X線診断装置、自走式CT装置などが内部に装備する電子機器類から放射するRF電磁波などが引き起こす電磁波ノイズの相互干渉を緩和するための対策及び外部に漏洩させないための対策、特に低漏洩電磁波対策、③M

R I の静磁場発生装置からの漏洩磁場、④手術室環境の高耐床荷重対策、⑤質量の大きな画像診断装置の搬入経路、搬入方法などを検討し、今年度から次年度を通して完成させる国立がんセンター中央病院9階手術室フロアにあらたな手術室構築のための具体的設計を実施し、施工を開始した。

今回の手術室構築の検討過程において、各種画像診断機器をRF電磁波シールド室内に設置することが非常に困難であることが明らかとなった。特に、オープンMRI装置には、元来撮像室内に引き込む各種信号線や傾斜磁場電流などを、すべてラインフィルタを通して供給する方策が確立している。しかし、同じ室内にX線診断装置やX線CT装置を設置すると、これらの電力線、信号線、制御線もすべてラインフィルタを経由して手術室内に供給する必要がある。しかしながら、これらの電力線、信号線、制御線は数百本にも達するものであり、これらをすべて動作確認して、機能や性能、並びに安定性を保証することは気の遠くなるような作業を繰り返す必要があり、現実的でないと判断した。

そこで、今回はX線診断装置とX線CT装置が同一の場所に設置されるので、これらをMRI撮像のためのシールドルームの外部に設置することとし、ラインフィルタの設置を不要とした。ただし、ここで手術室の有効利用のため、MRI室とX線診断装置およびX線CT装置とを同室に設置して使用することを想定するため、両者の間にRFシールドカーテンを用いて、MRI撮像時はカーテンを引き、X線診断装置あるいはX線CT装置を使用する際はカーテンを開くことで手術室の有効利用を考えた。

[II]内視鏡画像の歪補正に関して下記の結論を得た。

手術用ロボット装置のナビゲーションとして、内視鏡が持つ歪み量を抽出する評価手段として共線性の条件とヒルベルト変換を用いて、内視鏡画像歪み補正方法を確立した。また、術前に撮像した3次元MRI、CT画像などと重畳する際、歪補正後の内視鏡画像を重ね合わせる方法、およびMRI、CT画像を逆に内視鏡の歪に合わせるように逆補正を施し、内視鏡の画像に重ね合わせる方法の両方法を検討した。

[III] 手術用ロボット装置を開発するに際し、今回の開発の主要根幹部になる操作コンソールの基盤技術を開発した。グラフィカルユーザーインターフェイスを用いたユーザーの視認性の高い表示画面を開発した。

前節で述べた内視鏡歪補正技術を搭載し、術者が手術の全体像を把握しやすい操作コンソールを開発する予定である。3次元画像処理として一般的なMPR(Multi-Planar Reconstruction)、Curved MPR、3次元Volume Rendering、カットプレーン、仮想内視鏡機能(Virtual Endoscopy)などを装備するとともに、軟性内視鏡の先端部の位置認識を取り入れた断面表示機能を将来的に実現していく予定である。

また、臨床的には脳神経外科、胸部外科、乳腺外科、腹部外科、泌尿器外科などのさまざまな外科の術式を取り入れた手術プロトコルに対応できる柔軟性を実現するように操作コンソールの基盤技術の開発を継続するつもりである。

G. 研究発表

1. 論文発表

本年度は該当なし。

2. 学会発表

本年度は該当なし。

H. 知的財産権の出願・登録状況

1. 特許取得

本年度は該当なし。

2. 実用新案登録

本年度は該当なし。

3. その他

本年度は該当なし。

研究成果の刊行に関する一覧表

雑誌

発表者氏名	論文タイトル名	発表誌名	巻号	ページ	出版年
Tani K, <u>Kakizoe T</u> , et al.	Phase I study of autologous tumor vaccines transduced with the GM-CSF gene in four patients with stage IV renal cell cancer in Japan: Clinical and Immunological findings.	Mol Ther	10(4)	799-816	2004
Nakagawa T, Kanai Y, Ushijima S, Kitamura T, <u>Kakizoe T</u> , Hirohasi S	DNA hypomethylation on pericentromeric satellite regions significantly correlates with loss of heterozygosity on chromosome 9 in urothelial carcinomas.	J Urol	173	243-246	2005
<u>野村和弘</u>	患者さん主体の診療を念頭に、良好な医師患者関係の構築を 国際モダンホスピタルショウ2004/キーノートスピーチ「セカンドオピニオンの推進」から	Omnimanagement	10	16-20	2004
<u>野村和弘</u>	セカンドオピニオンの推進－患者さんとの信頼関係を育むために－	日本病院会雑誌	51(10)	1474-1490	2004
宮北康二、波井壮一郎、成田善孝、田部井勇助、 <u>野村和弘</u> 、横川めぐみ、大松重宏	国立がんセンター中央病院における終末期医療の現状 Current state of end-of-life care for the patients with malignant glioma in National Cancer Center Hospital.	Neuro-Oncol	14(1)	46-50	2004
Nomori H, <u>Kobayashi T</u> , et al.	Fluorine 18-tagged fluorodeoxyglucose positron emission tomographic scanning to predict lymph node metastasis, invasiveness, or both, in clinical T1 NO M0 lung adenocarcinoma.	J Thorac Cardiovasc Surg	128	396-401	2004
Kakinuma R, <u>Kobayashi T</u> , et al.	Progression of focal ground-glass opacity detected by low-dose helical computed tomography screening for lung cancer.	J Comput Assist Tomogr	28	17-23	2004
橋本隆二、金大永、波多伸彦、 <u>土肥健純</u>	経尿道的前立腺切除術のための管状組織低侵襲切除マニピュレータ	第2回生活支援工学系連合大会（第20回ライフサポート学会大会・第4回日本生活支援工学会大会）講演予稿集		123-124	2004

Hashimoto R, Kim D, Hata N, <u>Dohi T</u>	A tubular organ resection manipulator for transurethral resection of the prostate.	Proceedings of 2004 IEEE/RSJ International Conference on Intelligent Robots and Systems (IROS 2004)		3954-3959	2004
橋本隆二、金大永、松宮潔、波多伸彦、 <u>土肥健純</u>	経尿道的前立腺切除マニピュレータによる低侵襲切除システム	第13回日本コンピュータ外科学会大会・第14回コンピュータ支援画像診断学会大会合同論文集		73-74	2004
金季利、金大永、福与恒雄、松宮潔、小林英津子、波多伸彦、 <u>土肥健純</u>	ウェッジプリズムを用いた視野可変内視鏡の細径化<第1報>～視野欠損の低減に関する検討～	第13回日本コンピュータ外科学会大会・第14回コンピュータ支援画像診断学会大会合同論文集		127-128	2004
野口雅史、青木英祐、小林英津子、大森繁、村垣善浩、伊関洋、 <u>佐久間一郎</u>	脳外科用レーザー手術装置のための小型オートフォーカスシステムの開発	日本コンピュータ外科学会誌	6	印刷中	2005
Chui C, Kobayashi E, Chen X, Hisada T, <u>Sakuma I</u>	Combined compression and elongation experiments and non-linear modeling of liver tissue for surgical simulation.	Med Biol Eng Comput	42	787-798	2004
Aoki E, Suzuki T, Kobayashi E, Hata N, <u>Dohi T</u> , <u>Hashizume M</u> , <u>Sakuma I</u>	System architecture to reliable surgical robotic system.	Lect Note Comput Sci	3217	184-191	2004
Maruyama T, Muragaki Y, Tanaka M, <u>Iseki H</u> , <u>Sakuma I</u> , Hori T, Takakura K	Efficacy of 5-aminolevulinic acid-induced fluorescence detection in malignant glioma surgery.	Proc Comput Assist Radiol Surg (CARS 2004)		1290	2004
<u>佐久間一郎</u> 、朱志光、小林英津子、陳献、久田俊明	肝臓力学特性の実験的検討と構成式の導出	第13回日本コンピュータ外科学会大会／第14回コンピュータ支援画像診断学会大会合同論文集		225-226	2004

清水一秀、小林英津子、丸山隆志、村垣善浩、伊関洋、佐久間一郎	5-Aminolevulinic Acid誘導による蛍光画像を用いた術中脳腫瘍同定	第13回日本コンピュータ外科学会大会／第14回コンピュータ支援画像診断学会大会合同論文集		177-178	2004
青木英祐、鈴木孝司、小林英津子、波多伸彦、土肥健純、小西晃造、橋爪誠、佐久間一郎	CORBAを用いたプラットフォーム下におけるリアルタイム非同期通信によるパフォーマンスの評価	第13回日本コンピュータ外科学会大会／第14回コンピュータ支援画像診断学会大会合同論文集		157-158	2004
野口雅史、青木英祐、小林英津子、大森繁、村垣善浩、伊関洋、佐久間一郎	脳外科用レーザ手術装置のための小型オートフォーカスシステムの開発	第13回日本コンピュータ外科学会大会／第14回コンピュータ支援画像診断学会大会合同論文集		35-36	2004
古瀬慶博、砂田文宏、秋山朋之、八木昭彦、青木英祐、波多伸彦、佐久間一郎	CORBAを用いたネットワーク対応型医用機器の開発とLatencyの測定	情報処理学会研究報告	2004-EV A-8(9)	49-54	2004
元吉正樹、岡本淳、藤江正克	磁力駆動手術マニピュレータの開発	日本機械学会 [No. 04-4] ロボティクス・メカトロニクス講演会'04 講演論文集		2P2-H-54	2004
原田香奈子、坪内広太、千葉敏雄、藤江正克	Open-MRI下における低侵襲胎児手術用マニピュレータの開発	第13回日本コンピュータ外科学会論文集		111-112	2004
Harada K, Tsubouchi K, Chiba T, Fujie M G	Manipulators for intrauterine fetal surgery in an Open MRI.	ICRA 2005 IEEE Int Conf Rob Autom		Being Published	2005
Harada K, Tsubouchi K, Chiba T, Fujie M G	Manipulators for intrauterine fetal surgery in an Open MRI -Report on first prototype-	CARS 2005 Comput Assist Radiol Surg		Being Published	2005
原田香奈子、岩瀬健太郎、坪内広太、千葉敏雄、岸宏亮、藤江正克	Open MRI下胎児手術支援システムの開発（第一報）－微細マニピュレータと鉗子ナビゲーション－	ロボティクス・メカトロニクス講演会'06講演論文集		掲載予定	2005
伊関洋、村垣善浩、中村亮一、西澤幸司、大森繁、林基弘、堀智勝、高倉公朋	脳神経外科におけるRobotic Surgery	日本外科学会雑誌	105(12)	763-766	2004

伊関洋、村垣善浩、丸山隆志、中村亮一、南部恭二郎、大森繁、堀智勝、高倉公朋	神経外科領域の先端医療 インテリジェント手術室	神経研究の進歩	48(6)	860-866	2004
Hashizume M, Tsugawa K	Robotic surgery and cancer: the present state, problems and future vision.	Jpn J Clion Oncol	34(5)	227-337	2004
橋爪誠	手術支援ロボットの現状と未来	日本ロボット学会誌	22(4)	423-425	2004
橋爪誠	日本発手術ロボット開発の現状と未来:「臨床応用」	第13回日本コンピュータ外科学会大会/第14回日本コンピュータ支援画像診断学会大会合同論文集		281-282	2004
小西晃造、掛地吉弘、安永武史、家入里志、田上和夫、橋爪誠	マイクロサージェリーにおけるロボット手術システムの有用性の検討	第13回日本コンピュータ外科学会大会/第14回日本コンピュータ支援画像診断学会大会合同論文集		147-148	2004
鈴木優介、坂部啓、園田哲理、圓道知博、川上直樹、館暲	再帰性投影技術を用いたデスクトップ型バーチャル作業環境の研究	日本バーチャルリアリティ学会第9回大会論文集		129-132	2004
中山智量、北村喜文、岸野文郎	IllusionHoleにおける画像表示領域の重なり回避に関する検討	電子情報通信学会技術研究報告	104(489)	57-63	2004
岡島弘、北村喜文、上甲剛、岸野文郎	医療用を想定した多人数共有型立体表示装置の試作	電子情報通信学会技術研究報告			2005
Hachet M, Kitamura Y	3D interaction with and from handheld computers.	Proceedings of Workshop on New Directions in 3D User Interfaces		11-14	2005
中馬広一	骨盤内の軟部悪性腫瘍の手術	骨盤手術の最新手技		45-55	2004
中馬広一	進行性再発骨軟部肉腫に対する化学療法の現状	癌と化学療法	31(9)	1331-1339	2004
川井章、中馬広一、伊藤康正、山口洋、森本裕樹、別府保男	がん骨転移の疫学 (特集)	骨・関節・靭帯	17(4)	363-367	2004
川井章、別府保男、中馬広一、伊藤康正、山口洋、森本裕樹	シンポジウム 高齢者骨・軟部腫瘍の治療 高齢者骨・軟部腫瘍の治療成績-わが国の現状-	日本整形外科学会雑誌	78(7)	377-381	2004

<u>Kinoshita T</u>	Magnetic resonance imaging of benign phyllodes tumors of the breast.	Breast J	10	232-236	2004
<u>宮北康二</u>	脳の病気と脳腫瘍～脳腫瘍の診断と治療～	診療と新薬	41(12)	1237-1262	2004
<u>Oda I</u> , Gotoda T, Hamanaka H, et al.	Endoscopic submucosal dissection for early gastric cancer: Technical feasibility, operation time and complications from a large consecutive series.	Dig Endoscopy	17	54-58	2005
Takahashi A, Tsukamoto T, Tobisu K, Shinohara N, Sato K, Tomita Y, Komatsubara S, Nishizawa O, Igarashi T, <u>Fujimoto H</u> , et al.	Radical cystectomy for invasive bladder cancer: Results of multi-institutional pooled analysis.	Jpn J Clin Oncol	34	14-19	2004
<u>Kitamura H</u> , <u>Fujimoto H</u> , et al.	Dynamic computerized tomography and color doppler ultrasound of renal parenchymal neoplasms: correlations with histopathological findings.	Jpn J Clin Oncol	34	78-81	2004
Nakagawa T, Kanai Y, <u>Fujimoto H</u> , et al.	Malignant mixed epithelial and stromal tumours of the kidney: a report of the first two cases with a fatal clinical outcome.	Histopathology	44	302-304	2004
CANCER REGISTRATION COMMITTEE OF THE JAPANESE UROLOGICAL ASSOCIATION	Clinicopathological statistics on registered prostate cancer patients in Japan: 2000 report from Japanese Urological Association.	Int J Urol	12	46-61	2005
<u>藤元博行</u>	局所進行性前立腺癌に対するホルモン療法と手術療法の併用療法	日本臨床	63	271-278	2005
<u>藤元博行</u>	泌尿器科腫瘍外科の標準とすべき手技について(基調報告):総論	J Endourol		In press	2005
<u>Matsumura Y</u>	Phase I and pharmacokinetic study of MCC-465, a doxorubicin (DXR) encapsulated in PEG-immunoliposome, in patients with metastatic stomach cancer.	Ann Oncol	15	517-525	2004
Koizumi W, <u>Matsumura Y</u>	Phase I/II study of S-1 combined with cisplatin in patients with advanced gastric cancer.	Br J Cancer	89	2207-2212	2004
Hamaguchi T, <u>Matsumura Y</u>	Antitumor effect of MCC-465, pegylated liposomal doxorubicin tagged with newly developed monoclonal antibody GAH, in colorectal cancer xenografts.	Cancer Sci	95	608-613	2004

Okusaka T, <u>Matsumura Y</u>	New approaches for pancreatic cancer in Japan.	Cancer Chemother Pharmacol	54	78-82	2004
<u>Matsumura Y</u>	Phase I clinical trial and pharmacokinetic evaluation of NK911, a micelle-encapsulated doxorubicin.	Br J Cancer	91	1775-1781	2004
Bae Y, <u>Matsumura Y</u>	Preparation and biological characterization of polymeric micelle drug carriers with intracellular pH-triggered drug release property: Tumor permeability, controlled subcellular drug distribution, and enhanced in vivo antitumor efficacy.	Bioconjug Chem	16	122-130	2005
Hamaguchi T, <u>Matsumura Y</u>	NK105, a paclitaxel-incorporating micellar nanoparticle formulation, can extend in vivo antitumor activity and reduce the neurotoxicity of paclitaxel.	Br J Cancer		In press	2005

Phase I Study of Autologous Tumor Vaccines Transduced with the GM-CSF Gene in Four Patients with Stage IV Renal Cell Cancer in Japan: Clinical and Immunological Findings

Kenzaburo Tani,^{1,2,*} Miyuki Azuma,³ Yukoh Nakazaki,^{1,2} Naoki Oyaizu,¹ Hidenori Hase,¹ Junko Ohata,¹ Keisuke Takahashi,¹ Maki OiwaMonna,¹ Kisaburo Hanazawa,⁴ Yoshiaki Wakumoto,⁴ Kouji Kawai,⁵ Masayuki Noguchi,⁵ Yasushi Soda,¹ Reiko Kunisaki,¹ Kiyoshi Watari,¹ Satoshi Takahashi,¹ Utako Machida,¹ Noriharu Satoh,¹ Arinobu Tojo,¹ Taira Maekawa,¹ Masazumi Eriguchi,¹ Shinji Tomikawa,¹ Hideaki Tahara,¹ Yusuke Inoue,¹ Hiroki Yoshikawa,¹ Yoshitsugu Yamada,¹ Aikichi Iwamoto,¹ Hirofumi Hamada,⁶ Naohide Yamashita,¹ Koh Okumura,⁷ Tadao Kakizoe,⁸ Hideyuki Akaza,⁵ Makoto Fujime,⁴ Shirley Clift,⁹ Dale Ando,⁹ Richard Mulligan,¹⁰ and Shigetaka Asano¹

¹Advanced Clinical Research Center, The Institute of Medical Science, University of Tokyo, Tokyo 108-8639, Japan

²Department of Advanced Molecular and Cell Therapy, Division of Molecular and Clinical Genetics, Department of Molecular Genetics,

Medical Institute of Bioregulation, Kyushu University, Fukuoka 812-8582, Japan

⁴Department of Urology⁷ and Department of Immunology, Juntendo University School of Medicine, Tokyo 113-8421, Japan

⁵Department of Urology, University of Tsukuba School of Medicine, Ibaraki 305-8575, Japan

³Department of Molecular Immunology, Division of Oral Health Sciences, Graduate School, Tokyo Medical & Dental University, Tokyo 123-8519, Japan

⁶Department of Molecular Medicine, Sapporo Medical University, Sapporo 060-8556, Japan

⁸Department of Urology, National Cancer Center Hospital, Tokyo 104-0045, Japan

⁹Cell Genesys, Inc., South San Francisco, CA 94080, USA

¹⁰Division of Molecular Medicine, Children's Hospital, Department of Genetics, Harvard Medical School, Boston, MA 02115, USA

*To whom correspondence and reprint requests should be addressed at the Department of Advanced Molecular and Cell Therapy, Division of Molecular and Clinical Genetics, Department of Molecular Genetics, Medical Institute of Bioregulation, Kyushu University, 3-1-1, Maidashi, Higashi-Ku, Fukuoka-shi, Fukuoka 812-8582, Japan.
Fax: 81 92 642 6444. E-mail: taniken@bioreg.kyushu-u.ac.jp.

Available online 19 August 2004

We produced lethally irradiated retrovirally GM-CSF-transduced autologous renal tumor cell vaccines (GVAX) from six Japanese patients with stage IV renal cell cancer (RCC). Four patients received GVAX ranging from 1.4×10^8 to 3.7×10^8 cells on 6–17 occasions. Throughout a total of 48 vaccinations, there were no severe adverse events. After vaccination, DTH skin tests became positive to autologous RCC (auto-RCC) in all patients. The vaccination sites showed significant infiltration by CD4⁺ T cells, eosinophils, and HLA-DR-positive cells. The kinetic analyses of cellular immune responses using peripheral blood lymphocytes revealed an enhanced proliferative response against auto-RCC in four patients, and cytotoxicity against auto-RCC was augmented in three patients. T cell receptor β -chain analysis revealed oligoclonal expansion of T cells in the peripheral blood, skin biopsy specimens from DTH sites, and tumors. Western blot analysis demonstrated the induction of a humoral immune response against auto-RCC. Two of the four patients are currently alive 58 and 40 months after the initial vaccination with low-dose interleukin-2. Our results suggest that GVAX substantially enhanced the antitumor cellular and humoral

immune responses, which might have contributed to the relatively long survival times of our patients in the present study.

Key Words: GM-CSF, renal cell cancer, CD4⁺ T cell, CD8⁺ T cell, T cell repertoire

INTRODUCTION

Each year, approximately 3000 people die of renal cell cancer (RCC) in Japan [1]. Conventional treatments, such as surgery, chemotherapy, radiotherapy, and cytokine therapies, have not been established for stage IV RCC. Approximately 25% of RCC patients have metastatic disease at the time of diagnosis, and RCC sufferers have a reported 2-year survival rate of less than 20% [2]. As RCC is considered an immunogenic tumor, various types of antitumor immunotherapy have been reported that use cytokines, such as interleukin-2 (IL-2) and interferon- α ; cell therapy with LAK; or nonmyeloablative stem cell transplantation. As all of these therapies have their limitations, the introduction of more specific antitumor immunotherapy with less toxicity is required [2-8].

Granulocyte-macrophage colony-stimulating factor (GM-CSF)-secreting cancer cell vaccines, which are generated from cancer cells by *ex vivo* gene transfer, have been shown to elicit tumoricidal antitumor immune responses in a variety of animal models and in human clinical trials [9-11]. Irradiated GM-CSF-secreting cancer cell vaccines are thought to induce antitumor immune responses by recruiting antigen-presenting cells, such as dendritic cells (DCs), to the site of immunization. DCs, which are the most potent immunostimulatory antigen-presenting cells, are known to activate antigen-specific CD4⁺ and CD8⁺ T cells, by priming them with oligopeptides that are processed from the lethally irradiated dying cancer cells. The antitumor immune reaction induced by GM-CSF-transduced tumor cells has been reviewed previously [11].

Since the initial clinical report on the use of a GM-CSF gene-transduced tumor vaccine [10], there have been a number of clinical studies applying this technology to the treatment of melanoma, renal cell carcinoma, prostate cancer, pancreatic cancer, and non-small-cell lung cancer. All of these clinical studies were performed without any severe adverse events [12-22]. In a clinical study examining RCC, Simons *et al.* reported a randomized, double-blind dose-escalation study with equivalent doses of autologous, irradiated RCC vaccine cells, with or without *ex vivo* human GM-CSF gene transfer. GM-CSF gene-transduced vaccines were equivalent in toxicity to nontransduced vaccines up to the feasible limits of autologous tumor vaccine yield. There was no dose-limiting toxicity, no evidence of autoimmune disease, and no replication-competent

retrovirus encountered in 18 patients receiving full follow-up care. This phase I study demonstrated the feasibility, safety, and bioactivity of autologous GM-CSF gene-transduced tumor vaccines for RCC patients. An objective partial response was observed in one of the three patients who received 1.2×10^8 GM-CSF gene-transduced cells and showed the largest delayed-type hypersensitivity (DTH) conversion [13,14]. However, the optimum number of GM-CSF-transduced autologous renal tumor cell vaccine (GVAX) cells for use in vaccination and boosting and the optimum frequency of cell administration remain to be determined.

To determine more precisely whether GM-CSF-secreting RCC vaccines can be used safely to induce antitumor immunity in advanced RCC patients, we conducted a clinical trial of this treatment strategy. Our clinical protocol consisted of tumor resection by nephrectomy, the establishment of primary RCC cultures, and *ex vivo* gene transfer, which was carried out in our own cell-processing facility [23]. The minimum dosage of the vaccine cells was set according to the previous report on RCC by Simons *et al.* [14], and the booster schedule was based on a previous report on non-small-cell lung cancer by Soiffer *et al.* [16]. This was the first clinical trial of human gene therapy for cancer patients approved by the Japanese government and performed in Japan. The results of the present study indicate that this novel RCC immunotherapeutic regimen, which features vaccination with GM-CSF-secreting, irradiated autologous RCC tumor cells, is feasible, safe, and capable of eliciting systemic immune responses against RCC tumor cells. Furthermore, these patients, some of whom also received systemic low-dose IL-2 therapy, have been followed up on an outpatient basis.

RESULTS

Case Presentations

Forty patients suffering from either primary RCC with or without metastases or postoperative relapsed RCC were evaluated at our hospital between July 1998 and March 2001. Of these, 6 preoperative patients with stage IV RCC (UICC classification 1997) with metastatic lesions were allowed to participate in the present clinical study by our ethics committee, based on clinical condition and eligibility criteria listed under Patients and Methods. As

TABLE 1: Patient characteristics and clinical response to GVAX

	Patient			
	1	2	3	4
Age (years)/sex	60/male	71/male	57/female	50/male
Tumor site				
Primary	Right RCC	Right RCC	Left RCC	Left RCC
Metastases	Lung, liver	Sacral bone	Liver, lung	Lung
Previous therapy	None	Sacral irradiation	None	None
GM-CSF production ^a (ng/10 ⁶ cells/24 h)	49	98	51	116
No. of GVAX treatments	10	17	15	6
Vaccinated total cell number	2.2 × 10 ⁸	3.7 × 10 ⁸	3.2 × 10 ⁸	1.4 × 10 ⁸
Adverse events				
Systemic	Low-grade fever	Low-grade fever	None	None
Local	Erythema, pruritis	Erythema, pruritis	Erythema, pruritis	Erythema, pruritis, blister
Eosinophil number ^b (/μl; mean ± SD)	718 ± 76	437 ± 306	226 ± 283	390 ± 150
Clinical response	PD	SD	PD	PD, MR
Survival (months from first vaccination)	7.5 ^c	>62	45 ^c	>44

PD, progressive disease; SD, stable disease; MR, mixed response.

^a GM-CSF production rate from each autologous GM-CSF-transduced RCC.

^b Eosinophil number was measured 48 h after vaccination.

^c Patient passed away.

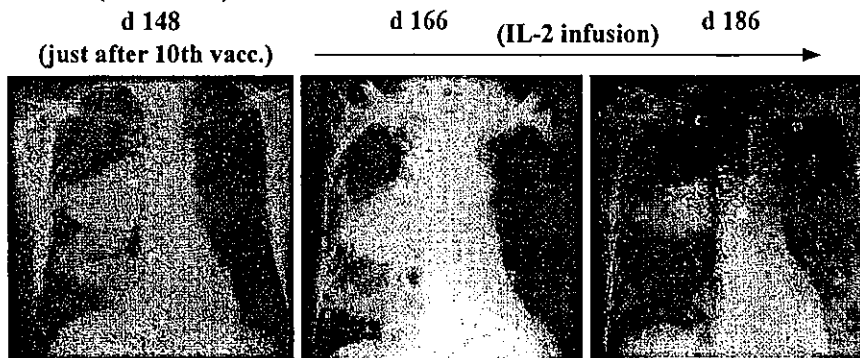
2 patients, a 48-year-old Japanese man having right RCC with multiple lung metastases and a 58-year-old Japanese man having right RCC with metastases to the right clavicle, bilateral lung, and liver, were excluded from this study because their GM-CSF-transduced RCC cells did not produce enough GM-CSF to satisfy the eligibility criteria as described under Autologous Vaccine Yield and Gene Transfer, 4 patients received GVAX.

The first patient (Case 1), a 60-year-old Japanese man, was diagnosed in August 1998 with RCC of the right kidney with multiple lung and liver metastases. His largest metastatic tumor, which was located in the right hilar region, was calculated volumetrically as 135 ml by computed tomography (CT) scan. The vaccine preparation used, his clinical course, and the autopsy findings have been reported previously [24]. Furthermore, he received a total of 2.2 × 10⁸ GVAX cells over 10 subcutaneous injections. The adverse events he experienced during vaccination are summarized in Table 1. He received gamma knife irradiation for his brain metastases and was initiated with low-dose (700,000–140,000 IU) recombinant IL-2 (rIL-2; Imunace, 350,000 IU/vial; Shionogi, Osaka, Japan), which was administered intravenously according to the patient's request. One week after the start of the rIL-2 treatment, the patient's right hilar mass lesion became smaller and decreased by 30% of the total volume within 1 month (Fig. 1A). Unfortunately, this patient died of multiple RCC metastases on July 8, 1999, 10 months after nephrectomy and 7 months after the start of GVAX vaccination (Fig. 2A).

The second patient (Case 2), a 71-year-old Japanese man, was diagnosed in December 1998 with a sacral

tumor that metastasized from RCC of the right kidney. He received a total dose of 30 Gy of irradiation of the sacral metastasis in February 1999 for severe pain, which was followed up with spinal anesthesia and oral morphine sulfate. The patient was nephrectomized on April 6, 1999, 43 days after the local irradiation, and pathology showed clear cell carcinoma. He received a total of 3.7 × 10⁸ GVAX cells in 17 subcutaneous injections from June 3, 1999, to February 3, 2000. The adverse events he experienced during vaccination are summarized in Table 1. His pain at the sacral area disappeared completely after the 5th vaccination, and oral morphine sulfate was discontinued. He experienced mechanical ileus due to nephrectomy after the 13th vaccination, which resolved after a few days of iv fluid treatment. The ileus was not related to the vaccination, and no recurrence of the ileus was noted after 4 further vaccinations. During the course of vaccination, the growth rate of the sacral tumor was stable as assessed by CT scan. His clinical course with the change in tumor size is described in Fig. 2B. The serum level of the nonspecific tumor marker immunosuppressive acidic protein returned from double the normal level to normal after the 6th vaccination, and a thallium scan showed decreased uptake of thallium at the tumor site on completion of the vaccination protocol (data not shown). Eleven months after the start of vaccination, pathological examination of the biopsied sacral bone specimen showed no RCC. This patient had been doing well without any treatment, with a performance status of zero, until he experienced a dull pain in his right femoral area in late November of 2001, 29 months after the 1st vaccination. He was diagnosed as having a 1-cm lytic metastasis in the right femoral bone. He received local

Case 1 (chest X-P)



Case 4 (CT)

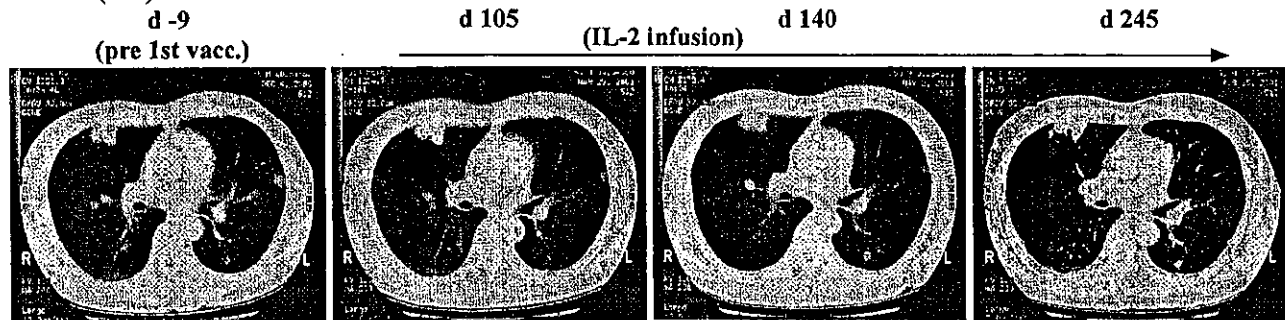


FIG. 1. Size change of the lung metastases in Cases 1 and 4 during the observation period after GVAX vaccination. (A) In Case 1, the size of the right hilar tumor, the largest metastatic lesion, became smaller after 1 week of low-dose IL-2 (d 166, day 166) and decreased by 30% after 1 month of low-dose IL-2 compared with the tumor just after the 10th vaccination. Chest X-ray films are presented. (B) In Case 4, the size of the left lung metastasis became smaller during vaccination as shown on two films for comparison between prevaccination and 105 days after the 1st vaccination. After the start of low-dose IL-2 between days 105 and 245, both the metastatic lesions in the left lung and those in the right lung became smaller. CT scan films are presented.

irradiation at a dose of 30 Gy to his femoral metastasis followed by daily low-dose rIL-2 (700,000–140,000 IU). His performance status at present, 58 months after the start of vaccination and with low-dose rIL-2 (350,000 IU) treatment, is zero.

The third patient (Case 3), a 57-year-old Japanese woman, was diagnosed in October of 1999 with RCC of the left kidney with multiple liver and lung metastases. She was nephrectomized on December 9, 1999, and the pathology showed clear cell carcinoma. She received a total of 3.2×10^8 GVAX cells in 15 subcutaneous injections, from February 22, 2000, to September 19, 2000. The adverse events she experienced during vaccination are summarized in Table 1. During the course of vaccination, the growth rate of the multiple liver tumors slowed, but the numbers and sizes of the masses did not decrease as assessed by CT scan (Fig. 2C). The sizes of the metastases in her right renal pelvis and lungs, observed on CT scan, were stable during vaccination. Her performance status was maintained at zero. After completion of the vaccination regimen, she requested systemic rIL-2 and interferon- α , but the cytokine treatments were discontinued due to the appearance of liver dysfunction, which resolved after discontinuation of cytokines. There-

after, she received monthly LAK (lymphokine-activated killer cells) therapy, upon her request. However, her metastatic lesions gradually increased, and she ultimately died of multiple RCC metastases on November 3, 2003, 47 months after nephrectomy and 45 months after the start of GVAX vaccination.

The fourth patient (Case 4), a 50-year-old Japanese man, was diagnosed in July of 2000 with right RCC with multiple lung metastases. He was nephrectomized on September 20, 2000, and pathology showed clear cell carcinoma. He received a total of 1.4×10^8 GVAX cells in six subcutaneous injections from December 13, 2000, to February 20, 2001. The adverse events he experienced during vaccination are summarized in Table 1. During the course of vaccination, the growth rate of the largest lung tumor slowed, and several tumors disappeared or were reduced in size, i.e., a mixed response was obtained. However, the sum of all the masses was increased, as assessed by CT scan. After the sixth injection, he was found to have a metastatic brain lesion with a maximum diameter of 1 cm, and the vaccination was discontinued according to our eligibility criteria. He received gamma knife irradiation to his brain metastasis and low-dose rIL-2 (700,000–140,000 IU) was initiated, which was given

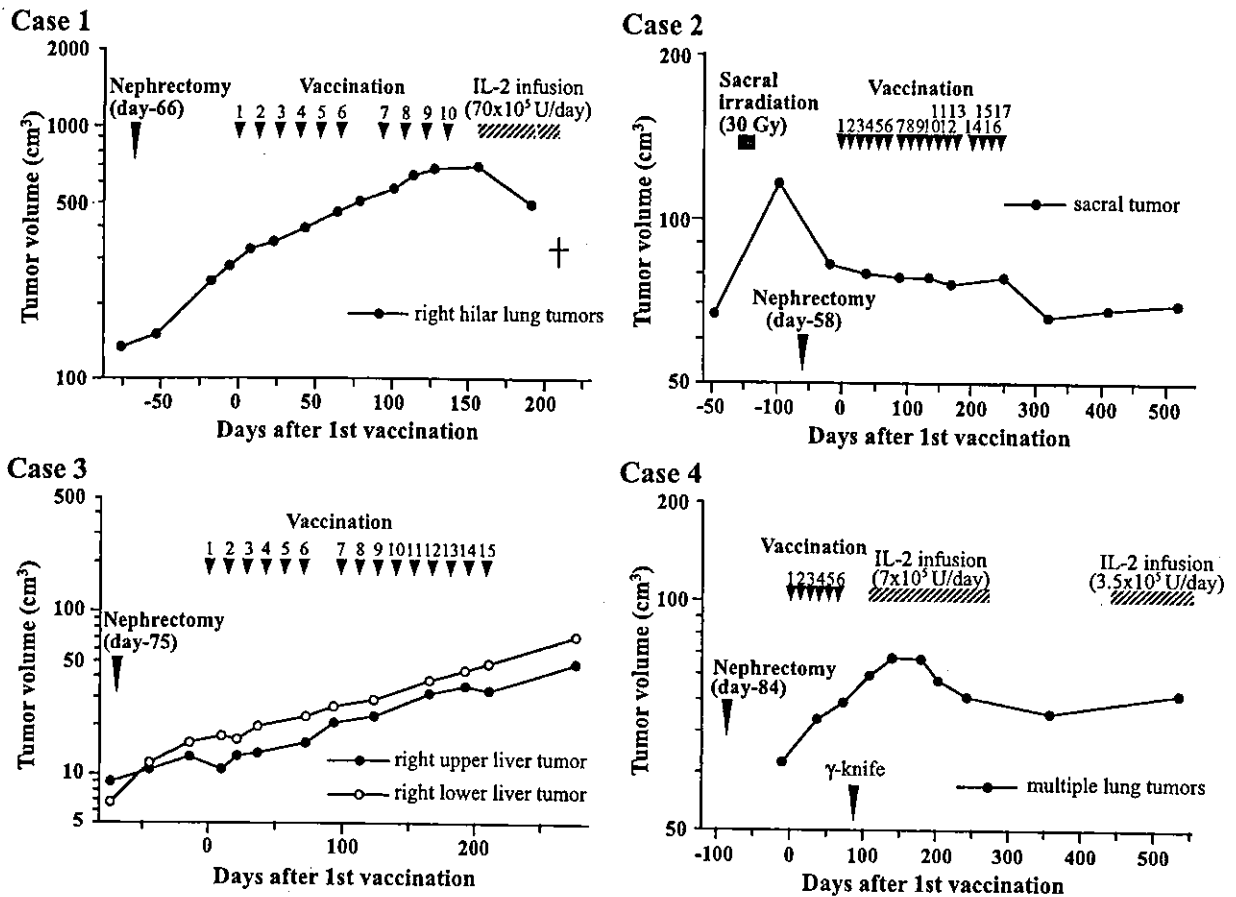


FIG. 2. Clinical summary of the four stage IV RCC patients (Cases 1 to 4) who received GVAX. The days of each vaccination are indicated by the short arrows, and the upper numbers signify the number of vaccinations. The long arrow indicates the time of nephrectomy of an RCC that involved the kidney. The tumor volume of each target metastatic lesion was measured periodically by CT scan or MRI. In Cases 1 and 4, low-dose IL-2 was administered after vaccination, upon request by the patients. The sacrum and brain were irradiated in Cases 2 and 4, respectively, to control sacral pain and brain edema.

subcutaneously, according to the patient's request. One month after the start of the rIL-2 treatment, the patient's total lung tumor volume was reduced and decreased to 30% of the peak volume over 3 months (Figs. 1B and 2D). His metastatic brain tumor was resected in January of 2002, and his performance status at present, 40 months after the start of vaccination and with low-dose rIL-2 (350,000 IU) treatment, is zero.

Autologous Vaccine Yield and Gene Transfer

In this trial, we generated the primary RCC cultures from large, advanced cancers with some areas of necrosis. The rate of successful vaccine cell expansion was 100% (6/6). In our preclinical models, the expression of paracrine GM-CSF by vaccine cells at levels higher than 40 ng/10⁶ cells/24 h induced antitumor immunity, and thus, we excluded cases producing less than this level from the present study [13,14]. A single transduction with MFGS-GM-CSF generated GM-CSF secretion levels of >40 ng/10⁶ cells/24 h in four of the six patients (66.6%) and

their production levels are shown in Table 1. The level of GM-CSF secretion by nontransduced cells ranged from 0 to 19 ng/10⁶ cells/24 h. We excluded two of the patients, who had GVAX production of only 20 and 12.4 ng/10⁶ cells/24 h, respectively, from our study. Cells from these individuals incorporated fewer copies of the integrated GM-CSF cDNA, and the cell doubling times were approximately two times greater than those of the cells producing >40 ng/10⁶ cells/24 h GM-CSF (data not shown). It is likely that the extended cell doubling times resulted in poor GM-CSF transduction efficiency in the two excluded cases.

Safety of Administration and Systemic Toxicities

All of the six patients' primary cultures met the vaccine cell yield specifications for at least six injections. Importantly, the tests for microbial contaminants gave negative results for all six GM-CSF-transduced products. All four patients, designated Cases 1, 2, 3, and 4, satisfied all of the eligibility criteria for this study and

received vaccinations (Table 1). No surgical complications were encountered that would preclude subsequent vaccination, although Case 1 had mechanical ileus 30 days after nephrectomy, which was before vaccination, and Case 2 had ileus 219 days after nephrectomy, between the 12th and the 13th vaccine injections. These symptoms were resolved by intravenous fluid replacement for several days. In the latter case, ileus was thought to be a late adverse event related to nephrectomy, but not vaccination because reinstitution of vaccination did not cause any other ileus symptoms. When vaccine yield and clinical status permitted, we performed multiple vaccinations for analysis of cumulative side effects. Cases 1, 2, 3, and 4 received GVAX at 66, 58, 75, and 84 days after nephrectomy, respectively. They received 48 fully evaluable, 14-day treatment cycles. Finally, Cases 1, 2, 3, and 4 received total cell doses of 2.2×10^8 , 3.7×10^8 , 3.2×10^8 , and 1.4×10^8 , respectively. During the vaccinations, we observed no hepatic, renal, pulmonary, cardiac, neurological, or gastrointestinal toxicities in any of the patients other than mechanical ileus in Case 2 as stated above. We observed significant increases in the numbers of peripheral blood eosinophils, but not other leukocytes, after immunization, as shown in Table 1, and the peak eosinophil level gradually increased in each case after repetitive vaccinations (data not shown). We did not observe the two most concerning toxicities, vaccine site-specific ulceration and development of acute autoimmune disease and, specifically, nephritis in uninephric patients, except in Case 4, who experienced blister formation at the vaccination site following the 6th vaccination (Table 1). We detected no RCR (replication-competent retrovirus) during the postvaccination follow-up period in any of the four patients who received the vaccine cells. The apparent lack of acute, systemic toxicity in this trial was paralleled by the lack of plasma elevation of GM-CSF in pharmacokinetic studies following treatment (data not shown). Follow-up observations for long-term toxicity, including autoimmune disease, have been under way on our two surviving patients, Cases 2 and 4, and no vaccine-related long-term toxicity has been noted to date.

Phenotype of Cells at the Sites of Vaccination

Although there was some individual variation, we noted significant infiltration by CD4⁺ T cells and eosinophils by day 30 (after the third vaccination); Case 3 had modest eosinophilic but intense mononuclear cell infiltration throughout the course of the vaccination protocol. Thereafter, these cell infiltrations were reduced in Cases 1 and 4, but increased in Cases 2 and 3. We could detect CD68⁺ macrophages and CD20cy-positive B cells as minor populations, but their levels were unaltered during the course of the vaccination protocol. The level of HLA-DR expression by infiltrating cells was

initially low, but increased by day 30. Intradermal S100⁺ dendritic cells were occasionally observed in most cases. These findings were comparable with previous reports [14–20].

Delayed-Type Hypersensitivity Reactions

DTH tests using Multitest CMI showed that Cases 1 and 3 had anergic scores and Cases 2 and 4 had normal scores, i.e., within the range seen for normal volunteers or patients with localized cancer (data not shown). As shown in Table 2, we did not observe significant DTH reactions (>10 mm) to unpassaged, irradiated autologous RCC cells in any of the four patients prior to treatment. Following vaccination, we observed significant DTH reactions in all patients and they were strongest after the sixth vaccination. We also observed DTH reactions to normal renal cells (NRCs), but these reactions were almost always smaller than those to RCC cells.

We examined pathological phenotypes and numerical analysis of the DTH reactions. In all four cases, significant DTH reactions against RCC were induced by days 24–28 (following the second vaccination), compared with the day 0 controls (prevaccination). CD4⁺ T cells were more dominant than CD8⁺ T cells at the sites of DTH reaction, followed by CD68⁺ macrophages and a few B cells, which was a common feature of DTH in all cases. We also observed various degrees of eosinophilic infiltration with degranulation. There were no significant differences between RCC and NRC with regard to the phenotypes of the cells in the DTH reaction, although more intense cell infiltration was observed against RCC than against NRC (data not shown). Although we detected significant DTH reactions until day 133 in Case 1, we observed a certain degree of attenuation in other cases.

Immunophenotypic Analysis of Tumor-Infiltrating Lymphocytes (TILs)

We performed immunophenotypic analysis of TILs for Case 1. Immunohistochemical analysis revealed that CD4⁺ T cells were the predominant infiltrating cell type in pretherapy primary tumors, followed by B cells (data not shown). Fig. 3 shows TILs in perivascular areas (Fig. 3A), around the foci of tumor cell apoptosis (Figs. 3B and D), and in an unremarkable area (Fig. 3D), within biopsied skin metastatic RCC specimens that were obtained 5 months after initiation of therapy. Regardless of the area under observation, the T cells in this specimen were CD8⁺, and we detected virtually no B cells. In addition, we observed increased numbers of CD68⁺ macrophages, especially around the apoptotic foci. In contrast to the results of the DTH test, we did not observe eosinophilic infiltration of the tumors (data not shown). Interestingly, immunophenotypic analysis of the infiltrating cells at the sites of surgically resected renal cancer and normal renal tissue, autopsied normal liver, lung, and kidney showed a predominance of

TABLE 2: Immunological findings in patients who received GVAX

	Patient			
	1	2	3	4
<i>Response to DTH skin test (mm)^a</i>				
Prevaccination	7 × 7/6 × 4.5	0 × 0/4 × 2	3 × 6/2 × 6	0 × 0/2 × 2
Peak reaction	85 × 65/30 × 35 (6) ^b	15 × 15/10 × 10 (6) ^b	25 × 25/2 × 1 (9) ^b	17 × 11/22 × 18 (6) ^b
<i>Lymphocyte proliferation (cpm)</i>				
Prevaccination	5,513	5,385	1402	1550
Post third	11,637	16,486	2836	6084
Post sixth	15,845	40,578	2442	6445
<i>Cytokine production (pg/ml)</i>				
<i>IFN-γ</i>				
Prevaccination	2746	UD	50	102
Post third	4952	199	481	UD
Post sixth	3568	394	967	UD
<i>IL-5</i>				
Prevaccination	UD	UD	395	128
Post third	1124	UD	863	1331
Post sixth	2088	792	1850	3017
<i>IL-10</i>				
Prevaccination	170	UD	UD	UD
Post third	80	UD	43	254
Post sixth	235	155	130	297
<i>Cytotoxicity assay (%)</i>				
Prevaccination	62.8	0.2	16.0	13.0
Post third	51.4	17.0	52.9	21.0
Post sixth	45.3	27.3	36.8	27.5
<i>TCR Vβ gene-segment repertoire analysis</i>				
	PB: 9,14,15,17 TIL: 10,17,21 DTH: 10,17	PB: 1,7,10,11,21 DTH: 1	PB: 4,18 DTH and Vac: 4,7	PB: 21,23 Vac: 9 DTH: 21

UD, under the detection level; PB, peripheral blood; TIL, tumor infiltrating lymphocytes; DTH, delayed type hypersensitivity.

^a DTH reactions were examined using cultured autologous RCC cells/normal renal cells as antigens.

^b The numbers in parentheses show that peak DTH reactions were observed after sixth or ninth vaccination.

CD4⁺ cells, whereas analysis at the sites of biopsied or autopsied tumor tissues obtained after vaccination or after vaccination followed by low-dose IL-2, respectively, showed a predominance of CD8⁺ cells (data not shown).

Vaccination Enhances the Proliferative Responses and Cytokine Production Against Autologous Tumors

We assessed the cellular immune responses using the peripheral blood mononuclear cells (PBMC) of patients who received GVAX. PBMC proliferated well in response to autologous RCC cell stimulation at all times tested (Table 2). In Case 2, the proliferative response observed before vaccination was augmented after vaccination. In all cases, vaccination markedly enhanced the proliferative responses to autologous RCC in the presence of IL-2. Especially, in Cases 2 and 4, those with prolonged clinically stable disease, the proliferative responses against autologous tumor cells remained high until the end of the study (data not shown).

IFN-γ in cultures stimulated with autologous RCC was enhanced after the initial vaccinations in Cases 1, 2, and 3, but not in Case 4 (Table 2). Conversely, IL-5 and IL-10 production was enhanced after vaccination in all cases. The enhancement of IL-5 seemed to correlate with the eosinophilia observed after the sixth vaccination. We also measured IL-4 production, but the levels of this cytokine were all below the limits of detection (data not shown).

Vaccination Induces Cytotoxicity Against Autologous RCC, Allogeneic RCC, and Autologous NRC

Case 1 showed comparatively high cytotoxicity against autologous RCC before vaccination. This level was maintained until after the fifth vaccination, after which it decreased. This was consistent with the higher DTH responses against autologous RCC and NRC seen in this case (Table 2). In Cases 2, 3, and 4, vaccination increased and maintained cytotoxicity against autologous RCC (Table 2, Fig. 4). Moreover, the addition of F(ab')₂ anti-CD3 mAb efficiently inhibited cytotoxicity against autologous RCC, suggesting the involvement

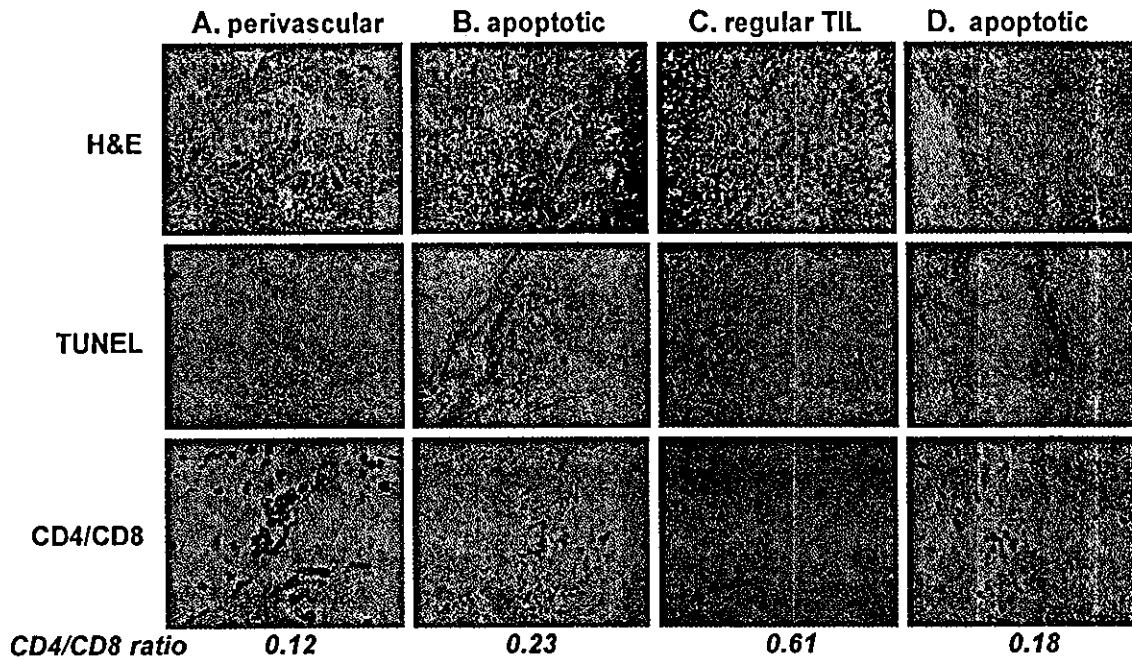
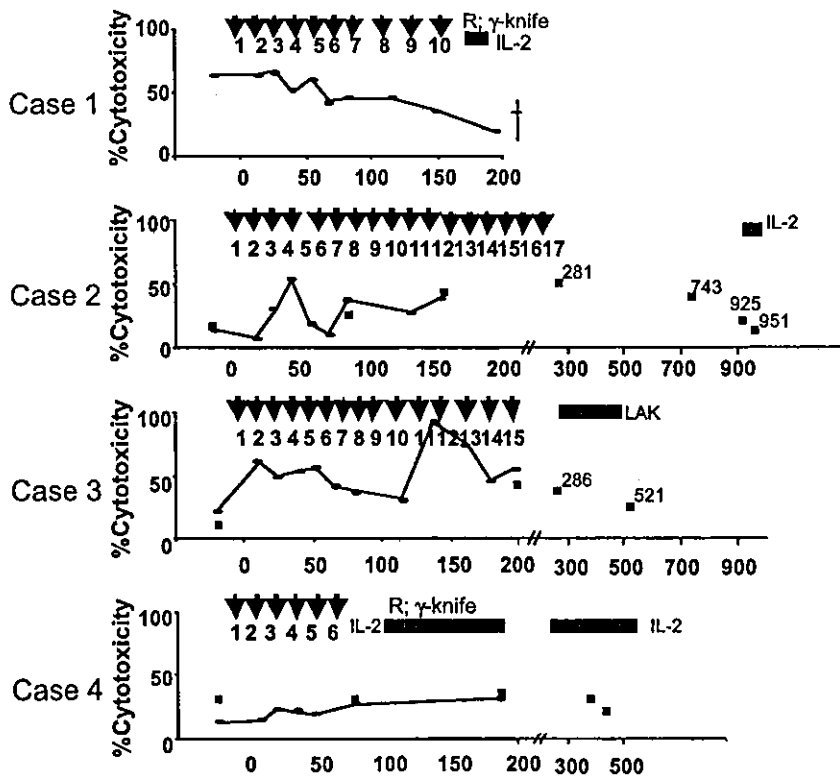


FIG. 3. Immunophenotypic analysis of tumor-infiltrating lymphocytes (TILs) in the RCC tumors of Case 1. TILs were observed in various areas, particularly (A) in the perivascular area, (B, D) around foci of tumor cell apoptosis, and (C) in unremarkable areas, within metastatic RCC that were obtained 7 months after the initiation of therapy. The T cell phenotype in this specimen had been converted to CD8 dominant, and few B cells were detected. To detect tumor apoptosis, the TUNEL method was applied as described under Patients and Methods.

FIG. 4. Cytotoxicity against autologous RCC in Cases 1 to 4. PBMC were cultured with irradiated GM-CSF-transduced autologous RCC in the presence of IL-2 for 7 days in 96-well microplates and ⁵¹Cr-labeled target cells were added. After a 6-h incubation, cytotoxicity was measured as described under Patients and Methods. Asterisks in the panels for auto-RCC targets show the cytotoxicity, which was inhibited by more than 25% by the addition of F(ab')₂ anti-CD3 mAb. Additional experimental values (squares) assessing the long-term results with additional treatment after the last vaccinations are also shown. IL-2, the rectangular bar represents the period of the administration of low-dose IL-2; R; γ -knife, gamma knife treatment was done for brain metastasis before the administration of IL-2.



of MHC-restricted T cell receptor (TCR)-mediated cytotoxicity.

TCR V β Clonotypic Analysis in DTH, Lung Metastasis, and RCC

In Case 1, we analyzed TCR V β gene usage in peripheral blood lymphocytes (2 days before vaccination and after the 6th and 9th vaccinations) and in tumor-infiltrated lymphocytes collected from tissue samples from the original surgically resected tumor, DTH skin biopsy (biopsied after the 4th vaccination), a metastatic skin lesion (biopsied after the 10th vaccination), and autopsied right hilar main lung metastases. We estimated the variation in the signal intensity by comparing the ratio of each V β signal observed in the regressed metastasized lung lesion with that observed in the nonregressed lung lesion or at the biopsied RCC or NRC DTH sites. The V β repertoire, which was overexpressed in the former sample, but not in the latter, was considered to indicate strong candidate T cell clones that were specifically induced by GVAX. In Case 1, we observed oligoclonal expansion of T cells with V β 9, 14, 15, and 17 repertoires in peripheral lymphocytes after the 9th vaccination (Fig. 5A). T cells with V β 10, 17, and 21 repertoires infiltrated the regressed tumor to a greater extent than the nonregressed tumor. These cells were also observed in the metastatic skin lesion (Fig. 5B). Interestingly, after vaccination, T cells with V β 10, 17, and 21 repertoires expanded clonally in the peripheral blood of Case 1, and the amplified TCR exactly matched those of the amplified fragments in a tumor-specific manner, namely T cells with V β 10 expanded dominantly in original tumor and lung metastasis, T cells with V β 17 in lung metastasis and much less in original tumor, and T cells with V β 21 in arm and lung metastasis and less in original tumor (Fig. 5C).

In Case 2, a T cell clone with V β 1 was increased in the pre- and postvaccination peripheral blood, nephrectomized tumor, biopsied sacral tumor, and DTH sites (Table 2). We saw oligoclonal expansion of T cells with V β 7, 10, 11, and 21 in peripheral lymphocytes after the vaccinations. Among them, T cell clones with V β 10, 11, and 21 expanded gradually after the first vaccination, and those with V β 7, 11, and 21 were also found in the nephrectomized original tumor.

In Case 3, the number of peripheral blood T cells with V β 18 was increased after the 6th, 9th, and 11th vaccinations and those with V β 4 were increased only after the 1st vaccination. Interestingly, T cells with V β 4 and 7 were increased at the RCC DTH sites after vaccination. These cells were also found at the vaccination site. T cells with V β 4 also infiltrated the metastasized liver tumor and nephrectomized original tumor.

In Case 4, peripheral lymphocytes contained increased numbers of T cells with V β 23 after the vaccinations. T cells with V β 9 were expanded after the sixth vaccination at the vaccinated site. T cells with V β 21 were expanded

at the RCC DTH sites. The results of the T cell repertoire analysis are summarized in Table 2.

Western Blotting

To examine whether the therapeutic regimen induced antitumor antibody responses in patients, we compared the serum antibody reactivity against autologous tumor cell lysates before and after initiating the therapy by immunoblot analysis. Using posttherapy serum as probes, high-molecular-weight proteins of around 250 kDa generated clear signals, whereas the pretherapy serum showed no or only weak signals at the same position (Fig. 6A), suggesting that the GVAX induced an antibody response in Cases 1, 2, and 4, while the results were less clear in Case 1. The signals appeared in similar positions in all patients, suggesting the presence of common antigens. These high-molecular-weight antigens were present in both tumor lysates and NRC lysates (Fig. 6A). In addition, human lip-derived fibroblasts might have identical antigens, while H69 lung cancer cells did not (Fig. 6B). Furthermore, the changes in the magnitude of the antibody immunoreactivity over time were analyzed using serum from Case 2. The strongest signal was observed in serum obtained 67 days after the initial vaccination, between the 5th and the 6th vaccinations. This response was maintained from day 67 until day 281, just after the 17th vaccination, and the immunoreactivity remained until the last time point examined at day 950 (Fig. 6C).

Clinical Outcomes

According to the standard clinical criteria, Case 2 was in stable disease, Case 4 was in mixed response, and Cases 1 and 3 were in progressive disease during the course of GVAX treatment (Table 1). As described under Case Presentations, Case 1 and Case 3 died of multiple metastases 7.5 and 45 months, respectively, after the first vaccination. Case 2 and Case 4 are alive 62 and 44 months, respectively, after the first vaccination in a stable condition with a performance status of zero. Interestingly, Case 1 with progressive disease and Case 4 with mixed response showed 30% decreases in their main or total lung metastatic lesions, respectively, 1 to 3 months after the start of low-dose IL-2 treatment (Figs. 2A, B, and 4).

DISCUSSION

Although the production of the GVAX from all six patients was successful, in two cases the levels of GM-CSF produced were not high enough for cell injection. Our production rate of 67% was compatible with previous reports [14–16]. The poor transduction efficiencies in our two patients were probably due to slowed proliferation of these RCC cells, as reflected by the extended doubling times. To overcome the heterogeneous transduction efficiency with retroviral vectors,

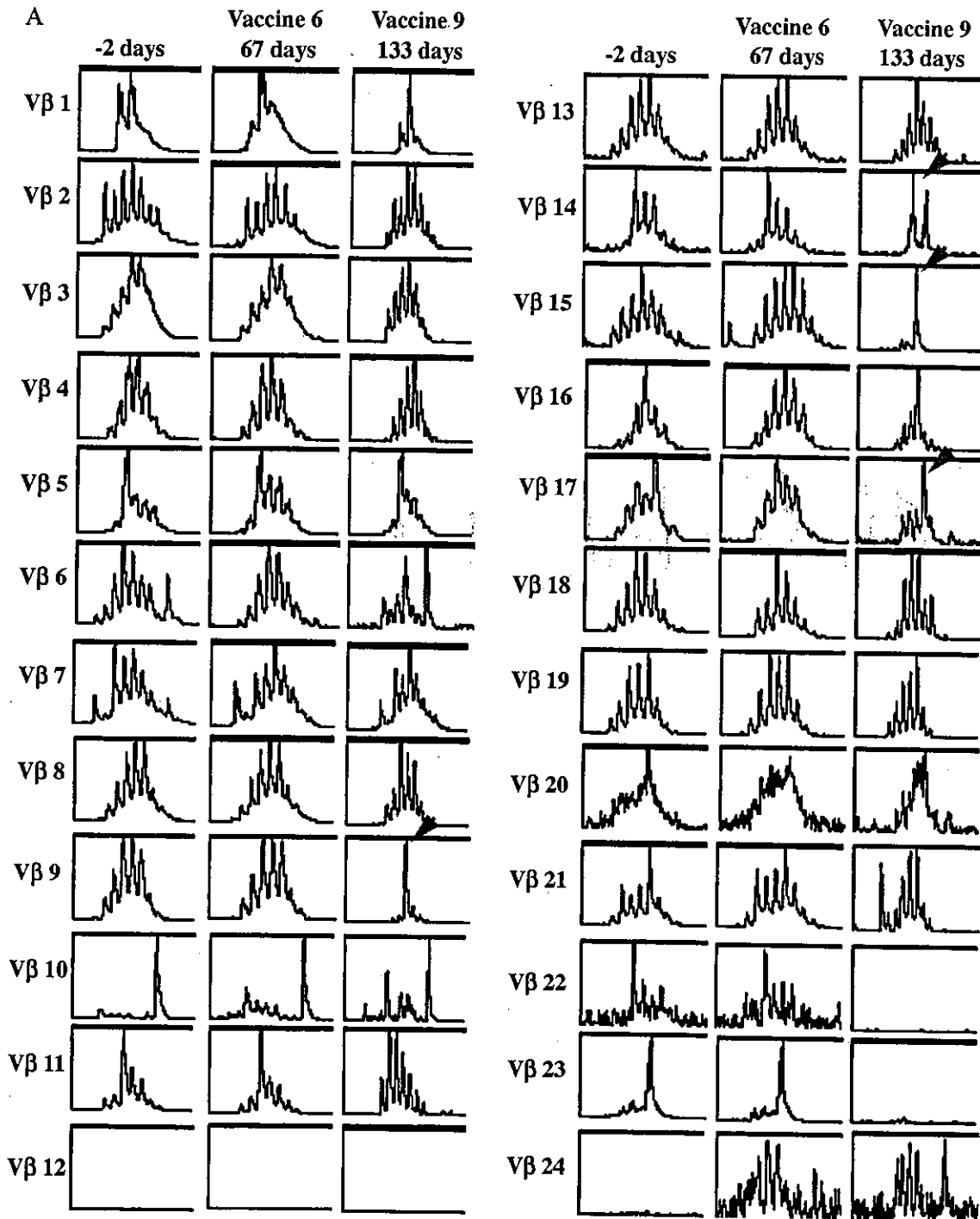


FIG. 5. TCR V β clonotypic analysis of the T cell infiltration in DTH, lung metastasis, and renal cell carcinoma in Case 1. (A) Oligoclonal expansion of T cell V β 9, 14, 15, and 17 repertoires was observed in peripheral lymphocytes after the ninth vaccination. (B) Larger numbers of T cells with V β 10, 17, and 21 repertoires infiltrated the regressed tumor than the nonregressed tumor. These cells were also observed in the skin metastasis designated Arm Meta. (C) After vaccination, T cells with V β 10, 17, and 21 repertoires were clonally expanded, and the amplified respective V β fragments exactly matched those of the amplified fragments in a tumor-specific manner.

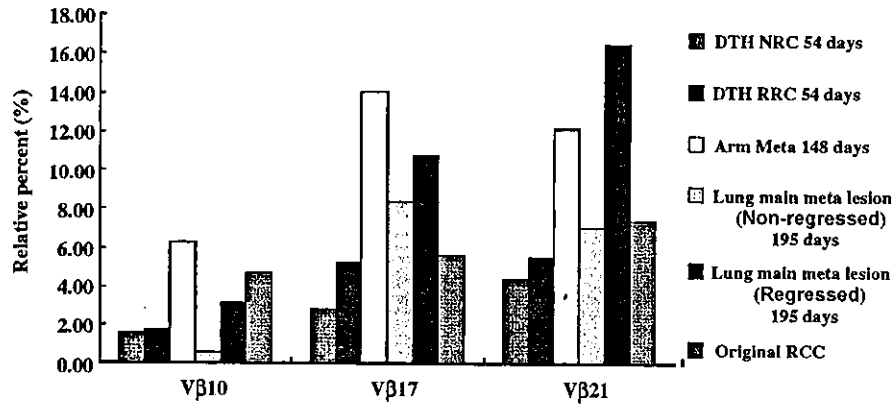
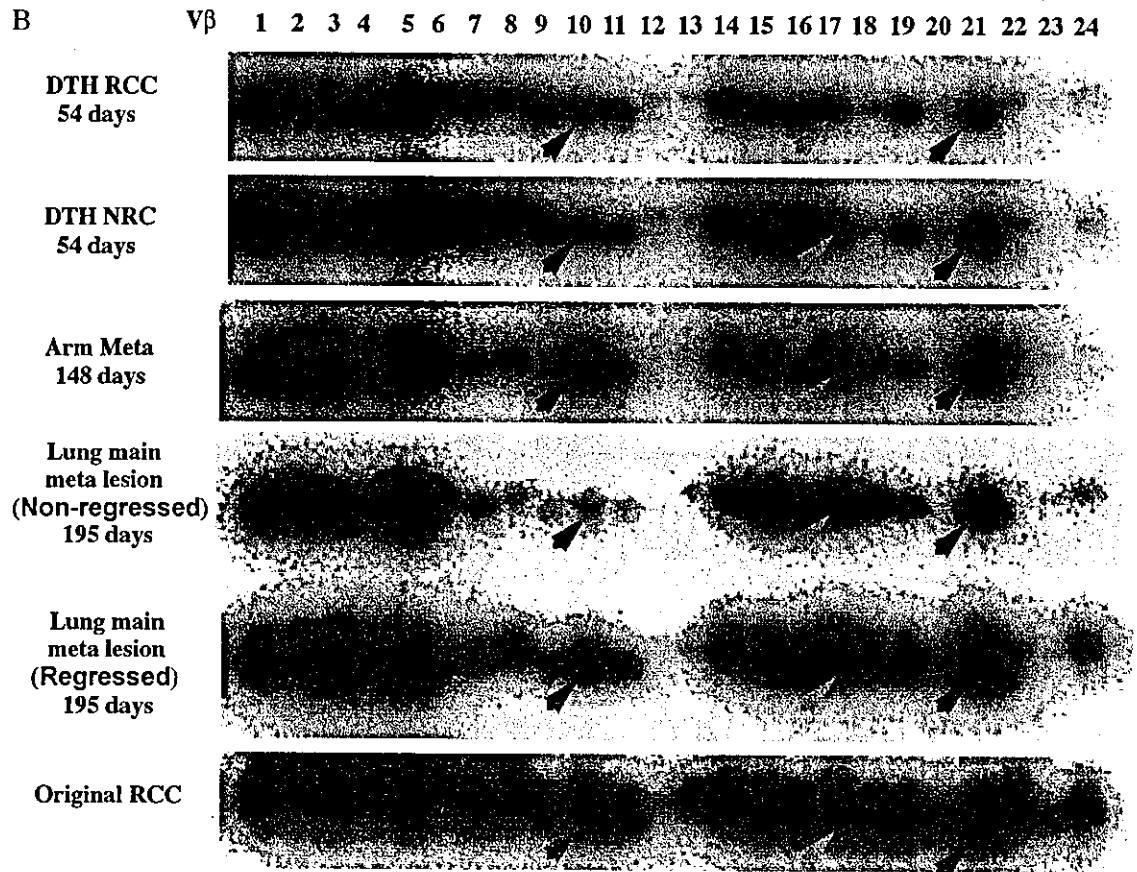


FIG. 5 (continued).

adoption of adenovirally transduced GM-CSF autologous tumor cells, allogeneic GM-CSF-transduced cell lines, or autologous tumor cell-based vaccines using GM-CSF-producing bystander cells should be examined as suggested previously [18–20,25–27].

We administered GVAX to four postnephrectomy patients with stage IV RCC without inducing severe vaccine-related adverse events. Furthermore, no remark-

able long-term adverse events have been observed in three patients, including two living patients. Our histological findings at the vaccination sites also support the previous observations of triggering the antitumor immune response at these sites [12,14–20,28]. DTH responses in Cases 1, 2, and 3 tended to show stronger reactions to autologous RCC cells than autologous NRC and suggested that anti-RCC-specific immunity was